Double-periodic Josephson junctions in a quantum dissipative environment

Tom Morel and Christophe Mora
Laboratoire de Physique de l'École Normale Supérieure, PSL Research University, Centre National de la Recherche Scientifique, Université Pierre et Marie Curie–Sorbonne Universités, Université Paris Diderot–Sorbonne Paris Cité, 24 rue Lhomond, 75231 Paris Cedex 05, France

(Received 16 July 2019; revised 27 October 2021; accepted 30 November 2021; published 17 December 2021)

Embedded in an ohmic environment, the Josephson current peak can transfer part of its weight to finite voltage and the junction becomes resistive. The dissipative environment can even suppress the superconducting effect of the junction via a quantum phase transition occurring when the ohmic resistance R_s exceeds the quantum resistance $R_\text{q} = h/(2e)^2$. For a topological junction hosting Majorana bound states with a 4π periodicity of the superconducting phase, the superconductor-insulator phase transition is shifted to $4R_\text{q}$. We consider a Josephson junction mixing the 2π and 4π periodicities shunted by a resistor, with a resistance between R_q and $4R_q$ such that the two periodicities promote competing phases. Starting with a quantum circuit model, we derive the nonmonotonic temperature dependence of its differential resistance resulting from the competition between the two periodicities, the 4π periodicity dominating at the lowest temperatures. The nonmonotonic behavior is first revealed by straightforward perturbation theory and then substantiated by a fermionization to exactly solvable models when $R_s = 2R_\text{q}$: the model is mapped onto a helical wire coupled to a topological superconductor when the Josephson energy is small and to the Emery-Kivelson line of the two-channel Kondo model in the opposite case. We also settle the *compact vs extended phase* controversy: introducing a compact phase variable across the junction, associated with a discrete charge, we rigorously prove that it is effectively replaced by an extended phase variable in presence of the environment.

DOI: 10.1103/PhysRevB.104.245417

I. INTRODUCTION

The tunneling of Cooper pairs in the Josephson effect can be reduced and even suppressed by a shunting resistance R_s. The resistor acts as an ohmic dissipative environment which controls the quantum fluctuations of the superconducting phase in the Josephson junction [1]. A renormalization group analysis predicts a quantum phase transition between a superconducting and an insulating state in a single Josephson junction [2–11]. The location of the quantum phase transition is determined solely by the dimensionless dissipation strength $\alpha = R_\text{q}/R_\text{s}$ where $R_\text{q} = h/(2e)^2$ is a quantum of resistance. When $\alpha > 1$, quantum fluctuations of the phase are suppressed by dissipation and the junction is superconducting. Conversely, for $\alpha < 1$, the dissipation is strong enough to destroy the Josephson current even at zero temperature. Several aspects of this transition have been observed experimentally [12–14] in superconducting junctions shunted by metallic resistors.

The model describing the quantum phase transition is well established and understood. It can be mapped onto the problem of quantum Brownian motion in a periodic potential which has been studied in detail [3,15,16]. It is also equivalent to the one-dimensional boundary sine-Gordon model [17] which describes in particular an impurity in a Luttinger liquid [18–20], such as a defect in an interacting nanowire or a point contact in a fractional quantum Hall state [21]. More generally, the quantum phase transition and environment fluctuations have a strong impact on the whole current-voltage characteristics of the junction at energies well below the gap [1,22–24].

The past years have witnessed a tremendous interest in the fractional Josephson effect in junctions hosting Majorana bound states [25,26]. Majorana excitations exhibit a topological protection against small perturbation and, as such, are believed to be building blocks for fault-tolerant quantum computation [27–29] via their braiding [30]. The fractional Josephson effect involves a 4π periodicity of the current as function of the superconducting phase in contrast with the usual 2π periodicity. It has been tested experimentally in semiconducting nanowires and topological junctions via the absence of odd Shapiro steps under radio-frequency irradiation [31–33]. Physically, the 4π periodicity is in fact associated with coherent single-electron tunneling at zero energy.

Topological junctions most probably combine Josephson energy terms with 2π and 4π periodicity. These multiple periodicities are nevertheless not uncommon since nonsinusoidal Josephson junctions, for instance in atomic point contacts [34,35], already involve different harmonics associated with the presence of Andreev levels. At zero energy, an Andreev state produces a 4π-periodic Josephson effect similar to the topological case. The presence of a strong Kondo impurity in the junction has been argued to pin the Andreev level to zero energy [36], thereby achieving a robust fractional Josephson effect. Moreover, there exist other means to realize different periodicities, including hybrid junctions involving superconducting and ferromagnetic layers which have been theoretically predicted to exhibit a controllable Josephson periodicity [37]. Another proposal is a specific arrangement of four Josephson junctions with a π periodicity called the

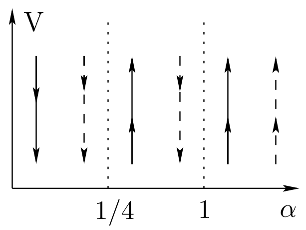

FIG. 1. Renormalization group scaling flows of the dissipative Josephson junction. V represents the strength of the potential term (E_J or E_M). The full lines represent the E_M term and the dashed lines represent the E_J term. For $\alpha > 1/4$, E_M is relevant. We therefore expect that the system is in an insulating state ($R = R_s$) for $\alpha < 1/4$ and in a superconducting state ($R = 0$) for $\alpha > 1/4$.

Josephson rhombus and also appearing in certain Josephson arrays [27,38–41].

In this paper, we study a Josephson junction having the two periodicities 2π and 4π shunted by an ohmic environment. Whereas we use here a full quantum treatment, the classical limit of this model has been investigated in the framework of the resistively capacitively shunted junction model with the purpose of describing Shapiro steps [42–45]. For a pristine topological Josephson junction with 4π periodicity, a renormalization group analysis [46] shows that the superconductor-insulator quantum phase transition is just shifted to the critical value $\alpha = R_q/R_s = 1/4$, four times smaller than for conventional Josephson junctions. This critical condition also reads $R_{q2}/R_s = 1$, with $R_{q2} = h/e^2$. It is then easily understood by noting that single-electron tunneling occurs through Majorana bound states in topological Josephson junctions in contrast to Cooper pair tunneling in conventional Josephson junctions.

In the presence of both periodicities, a competition emerges with the phase diagram shown in Fig. 1. We focus in this paper on the values of α between 1/4 and 1 where (i) the topological Josephson energy E_M, corresponding to single-electron tunneling, is relevant while (ii) the standard Josephson energy E_J, describing Cooper pair tunneling, is irrelevant but commensurate with the topological term. No intermediate fixed point can emerge from this competition since there are only two admissible infrared fixed points for the corresponding conformal field theory [47], representing the superconducting and insulating states. Nevertheless, the two terms can dominate different energy regimes, E_M being always the dominant effect at sufficiently low energy. We study the interplay of the two Josephson terms and the Coulomb interaction at arbitrary temperatures by using a combination of perturbative techniques and mappings to exactly solvable models for $\alpha = 1/2$. We compute the resistance of the whole system—Josephson junction and ohmic environment—as a function of temperature and exhibit nonmonotonic behaviors for different regimes of Josephson and charging energies.

We also emphasize that our theoretical modeling of the Josephson junction involves a phase variable that lives on a circle, i.e., a compact space, corresponding to a discrete charge transfer across the junction. Interestingly, in the presence of the dissipative environment, we are able to rigorously prove that this phase is effectively replaced by another extended [49,50] variable. We thereby recover the sine-Gordon model [2] used by many authors to discuss the superconductor-insulator transition. The issue of whether the phase should be considered as compact or extended has a long history [48–50] and has recently been disputed [51–53]. We solve this controversy by showing that the phase is decompactified by its coupling to the environment. Physically [54], the continuous delocalization of electrons to the environment suppresses charge quantization across the Josephson junction.

This paper is organized as follows: in Sec. II we use a quantum circuit description of the system and show that the dissipative term and charging energy can be absorbed in the Josephson tunneling to recover the usual sine-Gordon action [2,19]. The rest of the paper is devoted to the computation of the zero-bias differential resistance of the circuit at arbitrary temperature. In Sec. III, we identify the different low temperature regimes using renormalization group arguments. We then derive the resistance within linear response theory using perturbation theory and an infinite resummation based on refermionization at $\alpha = 1/2$, thereby showing the nonmonotonic temperature dependence. In Sec. IV, we treat with a tight-binding approach the limit of a deep Josephson periodic potential landscape with the Josephson energy much larger than the charging energy. A Bloch band description is combined with a refermionization procedure valid at $\alpha = 1/2$ to derive a mapping to the Emery-Kivelson model of the two-channel Kondo problem. The topological Josephson energy E_M acts as an effective magnetic field driving the system to a superconducting phase. We obtain an analytical form for the resistance as a function of temperature which qualitatively agrees with the shape derived in the opposite regime of small Josephson energies. We conclude in Sec. V.

II. CIRCUIT THEORY

A. Model

Instead of starting from an abstract Caldeira-Leggett form, we derive the relevant Hamiltonian from quantum circuit theory [55,56]. We consider the quantum device depicted in Fig. 2 composed of three parallel elements: a superconducting junction with a Josephson energy E_J, a second topological junction with a Josephson energy E_M, a capacitance C, and a resistor R_s. The whole apparatus is biased by a DC current I_0. The fractional Josephson junction allows for coherent single-electron tunneling, i.e., a 4π periodicity of the phase. We neglect in our analysis the quasiparticle excitations above the superconducting gap and we use $\hbar = k_B = 1$ for simplicity.

In the charge representation, the Hamiltonian of the system is

$$
\begin{aligned}
H = {} & \frac{1}{2C}\left(2e\hat{N} + \hat{Q} + \int_{-\infty}^{t} dt'\, I_0(t')\right)^2 + H_{R_s} \\
& - \frac{E_J}{2}\sum_n \Big(|n\rangle\langle n+1| + \text{H.c.}\Big) \\
& - \frac{E_M}{2}\sum_n \Big(|n\rangle\langle n+\frac{1}{2}| + \text{H.c.}\Big). \qquad (1)
\end{aligned}
$$

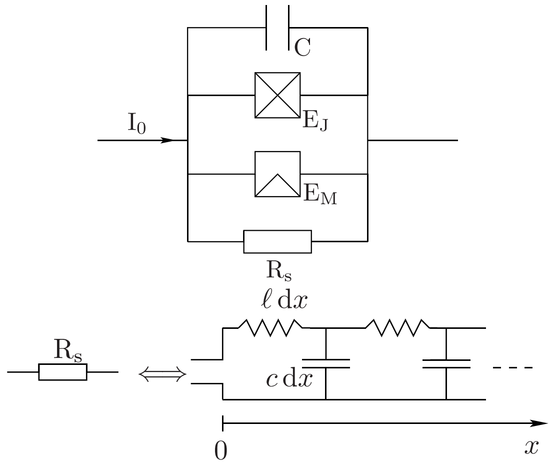

FIG. 2. (a) Schematic representation of a resistively and capacitively shunted Josephson junction combining 2π and 4π-periodic contributions. (b) Sketch of the distributed *LC* line circuit representing the shunt resistor R_s. The dissipative environment is described as a semi-infinite transmission line with lineic capacitance c and lineic inductance ℓ. The correspondence between the two representations gives $R_s = \sqrt{\ell/c}$.

The first term is the energy stored in the capacitance where the charge $2e\hat{N}$ across the Josephson junctions is added to the charge $\hat{Q}$ brought by the resistor and the charge integrated from the current source I_0. The third term corresponds to the Josephson tunneling between states with consecutive Cooper pair charge numbers, $\hat{N}\,|n\rangle = n\,|n\rangle$. The fourth term describes the tunneling of electrons through the topological Majorana fermions, implying that the charge operator $\hat{N}$ takes half-integer values, such that the corresponding phase operator

$$e^{i\hat{\varphi}/2} = \sum_n |n\rangle\langle n+1/2|, \tag{2}$$

with $[\hat{\varphi}, \hat{N}] = i$, is defined on a circle of size 4π. An electron is thus seen as half of a Cooper pair. H_{R_s} models the resistor in terms of a semi-infinite one-dimensional transmission line, i.e., as a collection of harmonic oscillators with lineic inductance ℓ and capacitance c [57]. The Hamiltonian H_{R_s} is

$$H_{R_s}[\{\hat{\phi}\},\{\hat{q}\}] = \int_0^{+\infty} dx\left[\frac{1}{2\ell}\left(\frac{\partial\hat{\phi}(x)}{\partial x}\right)^2 + \frac{\hat{q}(x)^2}{2c}\right] \tag{3}$$

where $R_s = \sqrt{\ell/c}$. The local flux $\hat{\phi}$ and the local charge $\hat{q}$ are conjugate variables and obey the canonical quantization

$$[\hat{\phi}(x), \hat{q}(x')] = i\delta(x - x'), \tag{4}$$

with the additional constraint that $\hat{Q}$ and $\hat{\phi}(0)$ are conjugate operators:

$$[\hat{\phi}(0), \hat{Q}] = i. \tag{5}$$

B. Unitary transformation

Before acting on the Hamiltonian (1), we note that the Hamiltonian $\hat{Q}^2/2C + H_R$ can be diagonalized by the mode expansion

$$\hat{\phi}(x) = \sqrt{\frac{R_s}{4\pi}}\int_0^{+\infty}\frac{d\omega}{\sqrt{\omega}}[a_{\mathrm{in},\omega}e^{-ikx} + a_{\mathrm{out},\omega}e^{ikx} + \mathrm{H.c.}], \tag{6a}$$

$$\hat{q}(x) = \frac{c}{i}\sqrt{\frac{R_s}{4\pi}}\int_0^{+\infty}\sqrt{\omega}\,d\omega[a_{\mathrm{in},\omega}e^{-ikx} + a_{\mathrm{out},\omega}e^{ikx} - \mathrm{H.c.}] \tag{6b}$$

with the dispersion $\omega = vk$ and the velocity $v = 1/\sqrt{\ell c}$, and the boundary conditions

$$a_{\mathrm{out},\omega} = \frac{1 + i\tau_s\omega}{1 - i\tau_s\omega}a_{\mathrm{in},\omega}, \qquad \hat{Q} = \frac{C}{c}\hat{q}(0), \tag{7}$$

corresponding to the reflection of microwaves by the capacitor. The commutation relations Eqs. (4) and (5) are recovered from the canonical quantization

$$[a_{\mathrm{in},\omega}, a^\dagger_{\mathrm{in},\omega'}] = \delta(\omega - \omega'). \tag{8}$$

This is a field theoretical description of a simple *RC* circuit with the time scale for discharge $\tau_s = R_s C$. Inserting this mode expansion, we find the diagonal form

$$\frac{\hat{Q}^2}{2C} + H_{R_s} = \int_0^{+\infty} d\omega\,\omega\,a^\dagger_{\mathrm{in},\omega}a_{\mathrm{in},\omega}. \tag{9}$$

In order to disentangle the different variables, it is convenient to apply the time-dependent unitary transformation

$$\hat{U} = \exp\left[i\hat{\phi}(0)\left(2e\hat{N} + \int_{-\infty}^t dt'\,I_0(t')\right)\right] \tag{10}$$

which essentially shifts the charge operator

$$\hat{U}\hat{Q}\hat{U}^\dagger = \hat{Q} - 2e\hat{N} - \int_{-\infty}^t dt'\,I_0(t'), \tag{11}$$

and acts as a displacement operator for the propagating modes

$$\hat{U}a_{\mathrm{in},\omega}\hat{U}^\dagger = a_{\mathrm{in},\omega} - i\sqrt{\frac{R_s}{\pi\omega}}\,\frac{2e\hat{N} + \int_{-\infty}^t dt'\,I_0(t')}{1 + i\tau_s\omega}. \tag{12}$$

We note however that $\hat{U}$ leaves $H_{R_s} = \hat{U}H_{R_s}\hat{U}^\dagger$ invariant. The transformed Hamiltonian $\tilde{H} = \hat{U}\,H\,\hat{U}^\dagger + i\partial_t\hat{U}\hat{U}^\dagger$ assumes the simplified form

$$\begin{aligned}\tilde{H} = &-\frac{E_J}{2}\sum_n(|n\rangle\langle n+1|e^{-2ie\hat{\phi}(0)} + \mathrm{H.c.})\\ &-\frac{E_M}{2}\sum_n\left(|n\rangle\langle n+\frac{1}{2}|\,e^{-ie\hat{\phi}(0)} + \mathrm{H.c.}\right)\\ &+\int_0^{+\infty}d\omega\,\omega\,a^\dagger_{\mathrm{in},\omega}a_{\mathrm{in},\omega} - I_0(t)\,\hat{\phi}(0),\end{aligned} \tag{13}$$

where the Cooper and single-electron tunneling terms are dressed by the dissipative phase functions $e^{\pm pie\hat{\phi}(0)}$, with $p = 1, 2$, describing the *RC* environment. Using Eq. (2), Eq. (13)

becomes

$$\tilde{H} = -E_J \cos(\hat{\varphi} - 2e\hat{\phi}(0)) - E_M \cos\left(\frac{\hat{\varphi}}{2} - e\hat{\phi}(0)\right) + \int_0^{+\infty} d\omega\, \omega\, a^\dagger_{\text{in},\omega} a_{\text{in},\omega} - I_0(t)\,\hat{\phi}(0). \tag{14}$$

At this point, $\hat{N}$ disappears and the phase operator $\hat{\varphi}$ commutes with the Hamiltonian $\tilde{H}$. $\hat{\varphi}$ is a constant of motion and it can be absorbed into $\hat{\phi}(0)$, i.e., removed from Eq. (14). Although we made no approximation, the charge discreteness and the related phase compactness no longer play a role in Eq. (14). We recover the standard sine-Gordon model [2] with an (noncompact) extended field despite our original choice of a compact Josephson phase. The phase $\hat{\varphi}$ has been effectively replaced by $\hat{\phi}(0)$ which includes the modes of the environment responsible for the suppression of charge quantization.

It is possible to formulate the Euclidean action corresponding to the Hamiltonian (14), where all modes except $\phi_0 \equiv 2e\hat{\phi}(0)$ are integrated,

$$S = \frac{1}{2\beta} \sum_{i\omega_n} \left(\frac{1}{8E_C} {\omega_n}^2 + \frac{\alpha}{2\pi} |\omega_n| \right) |\phi_0(i\omega_n)|^2 - E_J \int_0^\beta d\tau \cos\phi_0(\tau) - E_M \int_0^\beta d\tau \cos\left(\frac{\phi_0(\tau)}{2}\right), \tag{15}$$

for $I_0 = 0$. $\omega_n = 2\pi n T$ denotes a Matsubara frequency and $\beta = 1/T$ the inverse temperature. This expression recovers the standard action already used by many authors [2] for $E_M = 0$. We have introduced the charging energy $E_C = e^2/2C$ and the dimensionless dissipative constant $\alpha = R_\text{q}/R_\text{s}$ where $R_\text{q} = h/(4e^2)$ is the quantum resistance for Cooper pairs.

Hereinafter, we will use equivalently Eqs. (14) and (15) as a starting point to derive the differential resistance of our model.

III. DIFFERENTIAL RESISTANCE IN THE COULOMB BLOCKADE REGIME

A. Linear response theory

The effective resistance of the circuit is defined by the relation $V = R(T)\, I_0$ where I_0 is the bias current and the voltage drop across the junction is

$$V = \langle \partial_t \hat{\phi}(x = 0) \rangle,$$

where $\langle ... \rangle$ denotes the equilibrium expectation value. We use linear response theory to compute $R(T)$ by treating $-I_0(t)\,\hat{\phi}(0)$ in Eq. (14) as a perturbation. The details in the imaginary time formalism are provided in Appendix A where the expression

$$\frac{R}{R_\text{s}} = 1 + \frac{2\pi}{\alpha} \lim_{\omega\to 0} \text{Re}\left(\frac{i}{\omega} \lim_{i\omega_n \to \omega + i0^+} \int_0^\beta e^{i\omega_n \tau} \langle \hat{f}(\tau) \hat{f}(0) \rangle \right) \tag{16}$$

is derived. Re is the real part. We have also introduced the currentlike operator

$$\hat{f}(\tau) = E_J \sin[2e\,\hat{\phi}(\tau)] + \frac{E_M}{2} \sin[e\,\hat{\phi}(\tau)] \tag{17}$$

where we use the notation $\hat{\phi}(\tau) = \hat{\phi}(x = 0, \tau)$. For $E_M = E_J = 0$, we recover $R = R_\text{s}$ as expected.

The computation of the resistance (16) is based on the evaluation of the phase autocorrelation functions $\langle e^{ipe\,\hat{\phi}(\tau)}\, e^{-ipe\hat{\phi}(0)} \rangle$, with $p = 1, 2$. This can be done in perturbation theory in E_J, E_M, with the expression of the phase at $x = 0$,

$$\hat{\phi}(0) = \sqrt{\frac{R_\text{s}}{4\pi}} \int_0^{+\infty} \frac{d\omega}{\sqrt{\omega}} \left[\frac{2}{1 - i\tau_s\omega} a_{\text{in},\omega} + \text{H.c.} \right], \tag{18}$$

the thermal occupation

$$\langle a^\dagger_{\text{in},\omega} a_{\text{in},\omega'} \rangle = f_B(\omega)\delta(\omega - \omega'), \tag{19}$$

and the Bose factor $f_B(\omega) = (e^{\beta\omega} - 1)^{-1}$. The leading order $(E_J, E_M = 0)$ is given at zero temperature and in real time by the expression familiar to the $P(E)$ theory [1,35,58–60]

$$\langle e^{ipe\,\hat{\phi}(t)}\, e^{-ipe\,\hat{\phi}(0)} \rangle = e^{J(t,p)}, \quad J(t, p) = \frac{p^2}{2} \int_{-\infty}^{+\infty} \frac{d\omega}{\omega} \frac{\text{Re}Z(\omega)}{R_q} (e^{-i\omega t} - 1), \tag{20}$$

with the impedance of the RC environment $Z(\omega) = (i\omega C + 1/R_\text{s})^{-1}$.

Physically, the long-time asymptotics

$$e^{J(t,p)} \sim \left(\frac{\tau_s}{t}\right)^{p^2/2\alpha} \tag{21}$$

measures how fast phase correlations decay in real time. A large α corresponds to a slow diffusion indicating a well-defined superconducting phase. The result is that the second term with the time integral in Eq. (16) diverges as $\omega \to 0$ at zero temperature indicating a breakdown of perturbation theory and a flow towards zero resistance, i.e., a superconducting state with a Josephson current. In contrast, a small α gives a fast phase diffusion resulting in a vanishing second term in Eq. (16) for $\omega, T = 0$, i.e., an insulating state with $R = R_s$. Just by power counting, the threshold between these two states is found at $\alpha = p^2/4$, as recapitulated in Fig. 1.

B. Perturbation theory for the resistance

After setting the basis of the calculation in linear response theory, we compute the resistance at finite temperature from Eq. (16) and perturbatively in $E_J, E_M \ll E_C$. The leading corrections to the fully shunted junction are derived in Appendix B and expressed as [3]

$$\frac{R(T)}{R_\text{s}} = 1 - \frac{{E_J}^2}{2\alpha T^2} \int_0^{+\infty} dy\, e^{j_2(y, 2\alpha E_C/\pi^2 T)} - \frac{{E_M}^2}{8\alpha T^2} \int_0^{+\infty} dy\, e^{j_1(y, 2\alpha E_C/\pi^2 T)} \tag{22}$$

with the functions

$$j_p(y, a) = -\frac{p^2}{2\alpha} \left\{ \gamma + \Psi(a) + \ln 2 + \ln \text{ch}\left(\frac{y}{2}\right) + \frac{1}{2}\left[\frac{1}{a} + \frac{\pi\, e^{-ay}}{\sin(\pi a)}\right] \right.$$

$$- \frac{e^{-y}}{2}\left[\frac{1}{1-a}\,{}_2F_1(1,1-a,2-a,-e^{-y}) + \frac{1}{1+a}\,{}_2F_1(1,1+a,2+a,-e^{-y})\right]\Bigg\}. \quad (23)$$

γ is Euler's constant, Ψ the logarithmic derivative of the gamma function, and ${}_2F_1$ a hypergeometric function. The result (22) is only valid perturbatively, i.e., when the second and third terms are much smaller than 1. It can be further simplified at low temperatures $T \ll 2\alpha E_C/\pi^2$, leading to

$$\frac{R(T)}{R_s} = 1 - K_J\left(\frac{E_J}{E_C}\right)^2\left(\frac{T}{E_C}\right)^{-2+2/\alpha} - K_M\left(\frac{E_M}{E_C}\right)^2\left(\frac{T}{E_C}\right)^{-2+1/(2\alpha)} \quad (24)$$

with

$$K_J = \frac{\pi^{\frac{1}{2}+\frac{4}{\alpha}}\,\Gamma(\frac{1}{\alpha})}{(2\alpha)^{1+\frac{2}{\alpha}}\,(2e^{\gamma})^{\frac{2}{\alpha}}\,\Gamma(\frac{1}{2}+\frac{1}{\alpha})}, \quad (25a)$$

$$K_M = \frac{\pi^{\frac{1}{2}+\frac{1}{\alpha}}\,\Gamma(\frac{1}{4\alpha})}{4\,(2\alpha)^{1+\frac{1}{2\alpha}}\,(2e^{\gamma})^{\frac{1}{2\alpha}}\,\Gamma(\frac{1}{2}+\frac{1}{4\alpha})} \quad (25b)$$

with $\Gamma(x)$ the gamma function. We recover the results of the renormalization group analysis that E_J (resp. E_M) scales down to zero as the temperature is lowered for $\alpha < 1$ (resp. $\alpha < 1/4$) whereas it becomes increasingly large at low energy in the opposite case $\alpha > 1$ (resp. $\alpha > 1/4$).

We focus henceforth on the most interesting scenario where α is chosen between 1/4 and 1, such that E_M is relevant and E_J is irrelevant at low energy. There, a competition emerges between the two temperature corrections of Eq. (24) with opposite limits. Since E_M eventually dominates at sufficiently low energy, the competition is best discussed in the regime $E_M \ll E_J$. Differentiating $R(T)$ with respect to T, we find that the resistance reaches a (local) maximum for

$$\frac{T_m}{E_C} = \frac{4e^{\gamma}\alpha}{\pi^2}\left[\frac{(4\alpha-1)\,\tilde{\Gamma}(\alpha)}{16(1-\alpha)}\left(\frac{E_M}{E_J}\right)^2\right]^{2\alpha/3} \quad (26)$$

with $\tilde{\Gamma}(\alpha) = \Gamma(\frac{1}{4\alpha})\,\Gamma(\frac{1}{2}+\frac{1}{\alpha})/[\Gamma(\frac{1}{\alpha})\,\Gamma(\frac{1}{2}+\frac{1}{4\alpha})]$ and within the temperature range of validity of Eq. (24). For $T < T_m$ the resistance is an increasing function of temperature whereas it decreases for $T > T_m$. We note that the temperature correction due to E_M is diverging at zero temperature such that there is a temperature, much lower than T_m, below which the perturbative expansion (24) is insufficient.

For $T \sim E_C$, Eq. (24) is no longer valid; however we can set $E_M = 0$ in Eq. (22) since we assume $E_M \ll E_J$. The resulting expression for the resistance exhibits a (local) minimum. Although there is no closed analytical expression for the local minimum T^*, it can be expressed as

$$T^* = C(\alpha)\frac{2E_C}{\pi^2} \gg T_m \quad (27)$$

where the dimensionless coefficient $C(\alpha)$ is evaluated numerically and shown in Fig. 3.

The distance between the local maximum T_m and the local minimum T^* decreases with the ratio E_M/E_J. Quite generally for arbitrary E_M/E_J, the resistance can be obtained by

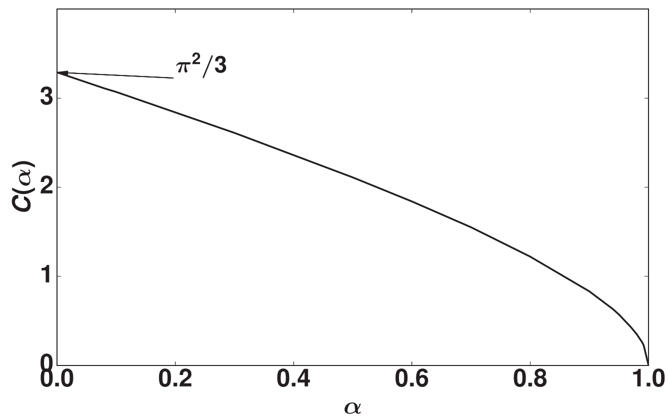

FIG. 3. $C(\alpha)$ vs the dimensionless dissipation term α. The function evolves between $\pi^2/3$ as $\alpha \to 0$ and zero as $\alpha \to 1$. This is in agreement with the result of Fisher and Zwerger [3].

a numerical evaluation of the integrals in Eq. (22). We thus observe a critical value of E_M/E_J, shown in Fig. 4 as function of α, at which the two extrema meet and disappear. Above this critical value, the resistance becomes a monotonic increasing function of the temperature. In practice, recent experiments on Shapiro steps [32,61] explored a wide range of values for E_J and E_C, and the ratio E_M/E_J between 10^{-3} and 10^{-1}. A higher value close to $E_M/E_J = 1/2$ has been reached in hybrid junctions combining superconducting and ferromagnetic layers [37].

C. Nonperturbative resummation

We mentioned in the preceding section that perturbation theory fails at low temperature since E_M multiplies a relevant operator. The description of the crossover to very low temperatures thus requires a resummation of the whole perturbation series, and such an exact resummation is not available for

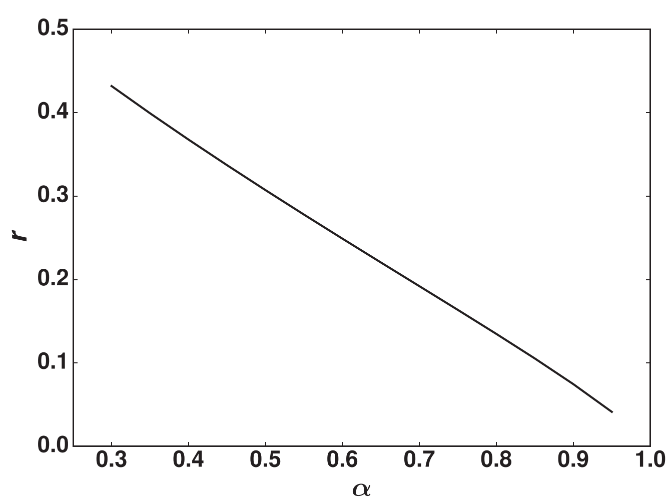

FIG. 4. Critical ratio $r = (E_M/E_J)_C$, as a function of α, at which the local maximum T_m and minimum T^* merge. Above, the resistance is a monotonous function of temperature (see also Fig. 5). The curve is close to linear and well fitted by $(E_M/E_J)_C = 0.605–0.590\,\alpha$.

general α when both E_J and E_M are nonzero. For $\alpha = 1/2$, however, a refermionization technique [19,62,63] has been successfully applied to compute the crossover for the resistance when $E_J = 0$. We extend it below to nonzero E_J where an exact crossover can also be formulated.

The main idea is to interpret $e^{ie\hat{\phi}}$ as a bosonized form of a fermion operator $\hat{\psi}$. At zero temperature, with a chiral Hamiltonian

$$H_0 = -i \int_{-\infty}^{+\infty} \hat{\psi}^\dagger(x)\, \partial_x\, \hat{\psi}(x) \tag{28}$$

the correlation function is

$$\langle \hat{\psi}^\dagger(x,t)\hat{\psi}(0,0)\rangle = \frac{1}{2\pi i(t-x)}. \tag{29}$$

At zero temperature and for $t \gg \tau_s = R_s C$, the integral (20) gives

$$\langle e^{ie\hat{\phi}(t,0)}\; e^{-ie\hat{\phi}(0,0)}\rangle \simeq e^{-i\pi/(4\alpha)} \times \left(\frac{\tau_s}{e^\gamma\; t}\right)^{1/(2\alpha)}. \tag{30}$$

For $\alpha = 1/2$, the correlator of $e^{ie\hat{\phi}}$ has the same time dependence as (29). The bosonization formula compatible with (30) and (29) is

$$\hat{\psi}(0) = \sqrt{\frac{e^\gamma}{\pi\tau_s}}\, \hat{a}\, e^{ie\hat{\phi}(0)}. \tag{31}$$

$\hat{a}$ is a local Majorana fermion with $\hat{a} = \hat{a}^\dagger$ and $\hat{a}^2 = 1/2$. $\hat{a}$ ensures the anticommutation rules for the fermionic field $\hat{\psi}(x)$. With the representation (31), the quadratic part of Eq. (14) can be replaced by the Hamiltonian (28), and

$$-E_M \cos(e\hat{\phi}(0)) = -\, r_M\, \hat{a}\, [\hat{\psi}(0) - \hat{\psi}^\dagger(0)]$$
$$\text{with} \quad r_M = E_M\sqrt{\frac{\pi\tau_s}{e^\gamma}}. \tag{32}$$

A straightforward point-splitting calculation connects $e^{2ie\hat{\phi}(0)}$ to $\hat{\psi}(0)\,\partial_x\hat{\psi}(0)$, since $\hat{\psi}(0)\hat{\psi}(0) = 0$ due to Fermi statistics. The two operators have scaling dimension 2 when $\alpha = 1/2$. The precise connection is obtained by identifying the two-point correlators using Eq. (29), with the result

$$-E_J \cos(2e\hat{\phi}(0)) = ir_J\, [\hat{\psi}(0)\,\partial_x\hat{\psi}(0) + \hat{\psi}^\dagger(0)\,\partial_x\hat{\psi}^\dagger(0)]$$
$$\text{with} \quad r_J = \frac{\pi{\tau_s}^2 E_J}{e^{2\gamma}}. \tag{33}$$

The refermionized Hamiltonian takes the form

$$H = -\,i\int_{-\infty}^{+\infty} \hat{\psi}^\dagger(x)\,\partial_x\,\hat{\psi}(x) - r_M\,\hat{a}[\hat{\psi}(0) - \hat{\psi}^\dagger(0)]$$
$$+\, ir_J\,[\hat{\psi}(0)\,\partial_x\hat{\psi}(0) + \hat{\psi}^\dagger(0)\,\partial_x\hat{\psi}^\dagger(0)], \tag{34}$$

which is quadratic and exactly solvable. This effective Hamiltonian allows for a complete resummation for energies smaller than E_C. Interestingly, Eq. (34) already appeared in a different context [64–68] as it can represent a semi-infinite helical wire—unfolded as a chiral mode on an infinite line—coupled at $x = 0$ to a topological superconductor hosting a single Majorana bound state at its edge. r_M plays the role of the tunnel coupling to the Majorana bound state while r_J generates Andreev reflections at the superconductor. In this model, an incoming electron can be reflected as an electron or a hole (and vice versa).

Equation (34) is easily diagonalized using a mode expansion [65,68] for $\hat{\psi}(x)$ and $\hat{\psi}^\dagger(x)$ summarized in Appendix C. Moreover, we can describe the relation between the left-moving electrons/holes ($x < 0$) and the right-moving electrons/holes ($x > 0$) with the S matrix. At the formal level, the second term in the expression (16) of the resistance, involving the correlator $\langle \hat{f}(\tau)\hat{f}(0)\rangle$, coincides with the differential conductance of the boundary helical model [65]. Hence, the resistance (16) can be expressed using one of the S-matrix components:

$$\frac{R}{R_s} = 1 - \int_{-\infty}^{+\infty} d\omega \left(-\frac{\partial n_f}{\partial\omega}\right) |S_{\rm ph}(\omega)|^2 \tag{35}$$

where $n_f(\omega) = (1 + e^{\beta\omega})^{-1}$ is the Fermi distribution and $S_{\rm ph}$ is the probability for an incoming electron with energy ω to be reflected as a hole. The derivation of $S_{\rm ph}$ is reproduced in Appendix C:

$$S_{\rm ph}(\omega) = \frac{i(2r_J\,\omega^2 + {r_M}^2)}{i{r_M}^2 + \omega\,(1 + r_J{r_M}^2 + {r_J}^2\omega^2)} \tag{36}$$

in agreement with Ref. [65]. Inserting Eq. (36) into Eq. (35), the effective resistance reads

$$\frac{R}{R_s} = 1 - F\left(\frac{4e^\gamma}{\pi^2}\,\frac{TE_C}{{E_M}^2}, \frac{\pi^5}{8e^{3\gamma}}\,\frac{{E_M}^2E_J}{{E_C}^3}\right) \tag{37}$$

where the dimensionless function $F(\tilde{T},\tilde{r})$ is given by

$$F(\tilde{T},\tilde{r}) = \int_{-\infty}^{+\infty} \frac{dx}{2{\rm ch}^2 x}\,\frac{(2\tilde{T}^2\,\tilde{r}\,x^2 + 1)^2}{1 + \tilde{T}^2x^2\,(1 + \tilde{r} + \tilde{T}^2\,\tilde{r}^2x^2)^2}. \tag{38}$$

For $E_J = 0$, the integration can be performed and we recover the known result [2,69]

$$\left.\frac{R}{R_s}\right|_{E_J=0} = 1 - \frac{\pi{E_M}^2}{4e^\gamma\,E_C\,T}\,\Psi'\left(\frac{1}{2} + \frac{\pi{E_M}^2}{4e^\gamma\,E_C\,T}\right). \tag{39}$$

At zero temperature, one obtains $F = 1$ consistent with a fully coherent Josephson junction. Let us emphasize that the result (37) was obtained assuming $T \ll 2E_C/\pi$ and $E_J, E_M \ll E_C$. As a consequence, we have ${E_M}^2E_J/{E_C}^3 \ll 1$ such that the second parameter $\tilde{r}$ in Eq. (38) is always much smaller than 1. At low temperature $T \ll {E_M}^2/E_C$, we can therefore ignore E_J to obtain the asymptotic expression

$$\frac{R(T)}{R_s} \simeq \frac{4e^{2\gamma}}{3\pi^2}\left(\frac{T}{{E_M}^2/E_C}\right)^2. \tag{40}$$

In the opposite limit $T \gg {E_M}^2/E_C$, we keep $\tilde{r} \sim E_J$ and recover the result Eq. (24) of the preceding section for $\alpha = 1/2$.

We plot in Fig. 5 the interpolation between Eqs. (37) and (22) for different values of $(E_M/E_C, E_J/E_C)$. We thus observe the crossover where the two extrema disappear.

IV. LARGE JOSEPHSON ENERGY

The analysis of Sec. III was restricted to the Coulomb blockade regime where the bare charging energy E_C is the largest energy scale. The Coulomb blockade tends to pin the

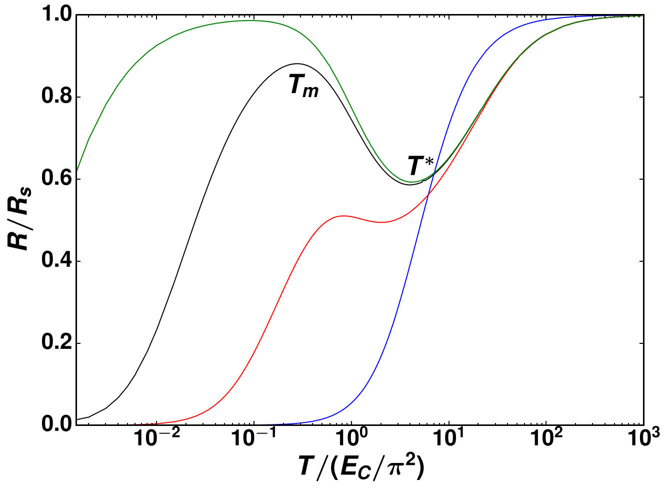

FIG. 5. Dimensionless resistance R/R_s as function of the reduced temperature $T/(E_C/\pi^2)$ for $\alpha = 1/2$ and different values of $(E_J/E_C, E_M/E_C)$ obtained by interpolation between Eqs. (37) and (22). We represent $(E_J/E_C, E_M/E_C) = (0.8, 0.1)$ (red line), (0.03,0.5) (blue line), (0.8, 0.006) (green line), and (0.8,0.03) (black line). The two extrema T_m and T^* merge at $E_J/E_M = 0.31$ (see Fig. 4).

superconductor charge which has the effect of delocalizing the conjugated phase variable. The shunted Josephson junction is then closer to an insulator, with a differential resistance below but in the vicinity of R_s, except at very low temperature where the relevant Josephson energy E_M takes over and reestablishes a dissipationless Josephson tunneling.

The resulting resistance, shown in Fig. 5, exhibits a local minimum at $T = T^* \sim E_C$ with a distance to the fully shunted junction $R = R_s$ increasing with E_J, reflecting a partial relocalization of the phase. This scaling suggests that the local minimum keeps decreasing with E_J/E_C until it reaches an almost vanishing resistance in a certain temperature range for E_J larger than E_C. In what follows, we consider directly the regime of deep potential wells $E_J \gg E_C$ while E_M is chosen below the plasma frequency $\omega_p = \sqrt{8E_J E_C}$.

We first diagonalize the model in the absence of the ohmic environment in Sec. IV A and then take in Sec. IV B $\alpha = 1/2$ where a mapping to the Emery-Kivelson model can be demonstrated. This gives the exact resistance for $\alpha = 1/2$ and a qualitative picture for α between 1/4 and 1, extending the analysis of Sec. III.

A. Dissipationless case

In the absence of dissipation, the Hamiltonian (1) simplifies as $H = H_0 - E_M \cos(\hat{\varphi}/2)$ with the transmon Hamiltonian [70]

$$H_0(n_g) = 4E_C\,(\hat{N} - n_g)^2 - E_J \cos\hat{\varphi} \tag{41}$$

where n_g is the offset charge of the capacitor. In the phase representation, $\hat{N} = i\partial_\varphi$ is acting on 2π-periodic functions, and H_0 can be diagonalized exactly using Mathieu functions [71]. For $E_J \gg E_C$, the energy of the ground state takes the suggestive form

$$E_0(n_g) = \frac{\omega_p}{2} - t_0 \cos(2\pi n_g), \tag{42}$$

where [70]

$$t_0 = 16\sqrt{\frac{E_J E_C}{\pi}}\left(\frac{E_J}{2E_C}\right)^{1/4} \exp\left(-\sqrt{\frac{8E_J}{E_C}}\right). \tag{43}$$

The ground state energy has a periodicity of 1 in n_g as expected from the discreteness of $\hat{N}$.

Although the above derivation is self-contained, it is instructive to formulate it using a Bloch band description [2,72]. The Hamiltonian H_0 (41) with the compact phase $\hat{\varphi}$ in $[0, 2\pi]$ is mathematically equivalent to solving $H_0(0)$ with an extended phase, i.e., $\hat{\varphi}$ between $-\infty$ and ∞, with n_g playing the role of the quasimomentum. In this language, Eq. (42) as function of n_g is a band dispersion. Focusing again on the regime $E_J \gg E_C$, the wave functions of low-energy eigenstates are strongly localized near the minima of the cosine potential and the Wannier function of the lowest band is the ground state of a harmonic oscillator,

$$W_0(\varphi) = \left(\frac{E_J}{8\pi^2 E_C}\right)^{1/8} \exp\left(-\frac{\varphi^2}{2}\sqrt{\frac{E_J}{8E_C}}\right), \tag{44}$$

with energy ω_p. The small overlap between consecutive Wannier functions induces a nearest-neighbor hopping term $t_0/2$. We thus obtain a tight-binding model the diagonalization of which reproduces Eq. (42) and t_0 is identified as the bandwidth of the lowest band in the cosine potential.

Next, we include E_M and numerically evaluate the spectrum of H. The presence of E_M doubles the size of the unit cell folding the spectrum at $n_g = \pm 1/2$, corresponding to single-electron tunneling, and opening gaps at the edge of the new Brillouin zone as illustrated in Fig. 6. In order to make further analytical progress, we consider $E_M < \omega_p$ such that the different bands of H_0 are not mixed, and project the Hamiltonian onto the lowest band. Due to nonzero E_M, the wave functions must have a periodicity of 4π in φ. For a given charge offset n_g, we find two such functions in the lowest band [73,74]:

$$\Psi_{\pm,n_g}(\varphi) = \sum_{p\in\mathbb{Z}} (\pm 1)^p\, W_0(\varphi - 2p\pi) e^{in_g(2p\pi - \varphi)} \tag{45}$$

with energies $E_0(n_g)$ and $E_0(n_g + 1/2)$. These are 4π-periodic functions, even and odd with respect to the parity operator $(-1)^{\hat{N}}\Psi_{\pm,n_g} = \pm\Psi_{\pm,n_g}$. After projecting the Hamiltonian H onto the basis (45), we get

$$H_{LE}(n_g) = t_0 \cos(2\pi n_g)\sigma_z + c_0 E_M \sigma_x + d_0 E_M \sigma_y \sin(2\pi n_g), \tag{46}$$

where σ_i $(i = x, y, z)$ are Pauli matrices operating in parity space and the constant term $\omega_p/2$ has been removed. This derivation of the different overlaps in Eq. (46) uses that $W_0(\varphi)$ takes appreciable values only close to $\varphi \simeq 0$. One consequence is that E_M does not enter the diagonal elements, or only with a very small contribution neglected here, whereas there is a perfect overlap $c_0 = 1$ along σ_x. The overlap along

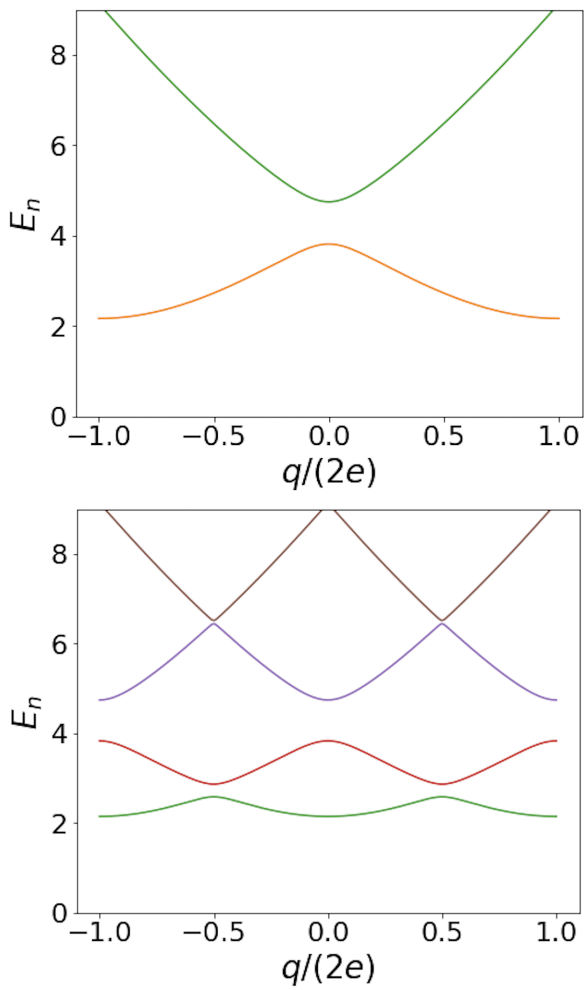

FIG. 6. Lowest bands obtained by a numerical solution of H as a function of the charge offset n_g in the absence of dissipation. The numerical solution is found [75,76] by performing a truncation in the charge basis $|n\rangle$ (eigenstates of $\hat{N}$) and diagonalizing a finite-size version of H. In both pictures, $E_C = 1$ and $E_J = 3$. Energies are given in units of the charging energy E_C. (a) Spectrum for $E_M = 0$. (b) Spectrum for $E_M = 3$. Gaps open at the edges of the reduced Brillouin zone.

σ_y is given by

$$d_0 = \frac{2^{1/3} t_0}{3^{-1/3}\omega_p}\sqrt{\frac{E_C}{E_J}}\,\Gamma\left(\frac{2}{3}\right) \ll 1, \tag{47}$$

and can be also neglected. The σ_x and σ_y components in Eq. (46) can be seen respectively as a staggered potential and a staggered hopping amplitude in the tight-binding model. We note that applying a nonzero flux between the two Josephson junctions can change the relative values of c_0 and d_0. The limiting case $c_0 = 0$ and $d_0 = 1$ corresponds to the Su-Schrieffer-Heeger model [77].

B. Effective Hamiltonian with dissipation

The projection to the lowest band of the extended potential can still be applied to the original Hamiltonian (1) provided the ohmic dissipation is not too strong. It amounts to an adiabatic approximation where one replaces the charge offset by $2en_g = -\hat{Q} - \int^t dt'\, I_0(t')$ in the transmon Hamiltonian H_0 (41). It is justified as long as the input current I_0 is weak and varies slowly in time, and if $\alpha^2 \ll 2\pi^2 E_J/E_C$ [16].

The projected Hamiltonian is

$$H_P = H_{LE}\left(\frac{\hat{Q}}{2e} + \frac{Q_0(t)}{2e}\right) + H_{R_s}, \tag{48}$$

where $Q_0(t) = \int^t dt'\, I_0(t')$, which we expand to first order in Q_0 as

$$H_P \simeq H_{LE}\left(\frac{\hat{Q}}{2e}\right) + H_{R_s} - t_0 \frac{\pi Q_0(t)}{e} \sin\left(\frac{\pi \hat{Q}}{e}\right), \tag{49}$$

and, for $Q_0 = 0$,

$$H_P = t_0 \cos\left(\frac{\pi}{e}\hat{Q}\right)\sigma_z + E_M\,\sigma_x + H_{R_s}. \tag{50}$$

Due to the absence of the capacitive term, the mode expansion of the fields in the transmission line differs slightly from Sec. II B and we have

$$\hat{\phi}(0) = \sqrt{\frac{R_s}{4\pi}} \int_0^{\omega_p} \frac{d\omega}{\sqrt{\omega}}\left[\frac{2}{1 - i\tau_0\omega}\, a_{\text{in},\omega} + \text{H.c.}\right], \tag{51a}$$

$$\hat{Q} = \frac{1}{\sqrt{4\pi R_s}} \int_0^{\omega_p} \frac{d\omega}{\sqrt{\omega}}\left[\frac{-2i\tau_0\omega}{1 - i\tau_0\omega} a_{\text{in},\omega} - \text{H.c.}\right], \tag{51b}$$

where τ_0 is a regularizing time that is eventually sent to infinity. Frequencies are cut off at the plasma frequency ω_p at which higher bands start to play a role. The correlator $K_{\hat{Q}}(t) = \langle e^{i\pi\hat{Q}(t)/e} e^{-i\pi\hat{Q}(0)/e}\rangle$ describes now charge fluctuations. At zero temperature, one gets

$$K_{\hat{Q}}(t) = \exp\left[2\alpha \int_0^{\omega_p} \frac{d\omega}{\omega} \frac{(\tau_0\omega)^2}{1 + (\tau_0\omega)^2}(e^{-i\omega t} - 1)\right], \tag{52}$$

or, for $1/\omega_p \ll t \ll \tau_0$ and α, $K_{\hat{Q}}(t) \sim 1/(\omega_p t)$. The same fermionization as Eq. (31) can be performed such that

$$t_0 \cos\left(\frac{\pi}{e}\hat{Q}\right) = r_0\, \hat{a}[\hat{\psi}(0) - \hat{\psi}^\dagger(0)] \tag{53}$$

with $r_0 \sim t_0/\sqrt{\omega_p}$. The Hamiltonian (50) can be further transformed using the representation of Pauli matrices in terms of Majorana fermions [78], i.e., $\sigma_x = i\eta_2\eta_3$, $\sigma_y = i\eta_3\eta_1$, and $\sigma_z = i\eta_1\eta_2$. The commutation relations of the Pauli matrices are ensured by the Clifford algebra $\{\eta_i, \eta_j\} = 2\delta_{ij}$. Using these representations, the Hamiltonian (50) becomes

$$\begin{aligned} H_P = &-i\int_{-\infty}^{+\infty} \psi^\dagger(x)\partial_x\psi + iE_M\,\eta_2\eta_3 \\ &- ir_0\,[\hat{\psi}(0) - \hat{\psi}^\dagger(0)]\,\hat{a}\,\eta_1\eta_2. \end{aligned} \tag{54}$$

$\hat{a}\,\eta_1$ commutes with H_P such that we can choose $\hat{a}\eta_1 = i/\sqrt{2}$ and

$$\begin{aligned} H_P = &-i\int_{-\infty}^{+\infty} \psi^\dagger(x)\partial_x\psi + iE_M\,\eta_2\eta_3 \\ &+ \frac{r_0}{\sqrt{2}}[\hat{\psi}(0) - \hat{\psi}^\dagger(0)]\,\eta_2. \end{aligned} \tag{55}$$

This Hamiltonian coincides exactly with the effective model found by Emery and Kivelson [79,80] to solve the two-channel Kondo model in the presence of a magnetic field. r_0

is a relevant operator driving the system to a strong-coupling fixed point where r_0 is large—or E_J is large—and the Majorana fermion η_2 is screened. The effect of the magnetic field $\approx E_M$ is to stop the renormalization group flow. Equation (55) is quadratic and therefore analytically solvable.

C. Resistance

The voltage drop across the junction is

$$\begin{aligned} V &= \langle \dot{\hat{\phi}}(t)\rangle = i\langle [H_P, \hat{\phi}]\rangle \\ &= -t_0 \frac{\pi}{e}\langle \sin\left(\frac{\pi}{e}\hat{Q}\right)\sigma_z\rangle + i\langle [H_{R_s}, \hat{\phi}]\rangle \end{aligned} \tag{56}$$

where we use again the notation $\hat{\phi}(t) = \hat{\phi}(x=0,t)$. The second term $[H_{R_s}, \hat{\phi}]$ gives zero. Using the Kubo formula and Eq. (49) for the linear coupling to the bias current, we obtain the expression for the resistance:

$$\frac{R(T)}{R_s} = 2\pi\,\alpha \lim_{\omega\to 0} \mathrm{Re}\Big(\frac{i}{\omega} \lim_{i\omega_n\to\omega+i0^+} \int_0^\beta e^{i\omega_n\tau}\,\langle \hat{g}(\tau)\hat{g}(0)\rangle\Big) \tag{57}$$

where

$$\begin{aligned} \hat{g}(\tau) &= it_0 \sin\left(\frac{\pi}{e}\hat{Q}(\tau)\right)\eta_1(\tau)\,\eta_2(\tau) \\ &= -i\frac{r_0}{\sqrt{2}}[\hat{\psi}(\tau) + \hat{\psi}^\dagger(\tau)]\,\eta_2(\tau) \end{aligned} \tag{58}$$

where $\hat{\psi}(\tau) = \hat{\psi}(\tau, x=0)$. Using the S-matrix formalism introduced in the previous section with Eq. (54), we finally obtain

$$\frac{R(T)}{R_s} = \int_{-\infty}^{+\infty} d\omega \left(-\frac{\partial n_f}{\partial\omega}\right)\frac{{r_0}^4\,\omega^2}{(\omega^2 - 4{E_M}^2)^2 + {r_0}^4\,\omega^2}. \tag{59}$$

For $E_M = 0$, one obtains [69]

$$\frac{R}{R_s} = \frac{{r_0}^2}{2\pi T}\,\Psi'\Big(\frac{1}{2} + \frac{{r_0}^2}{2\pi T}\Big) \tag{60}$$

with the infrared insulating fixed point, $R = R_s$, at zero temperature.

A nonzero E_M drastically changes to the infrared superconducting fixed point. Equation (59) gives the resistance $R = 0$ at zero temperature. The temperature dependence of the resistance is shown in Fig. 7 by evaluating the integral in Eq. (59). For $T \gg E_M$, the integral simplifies as

$$\frac{R}{R_s} \simeq \frac{\pi}{4}\frac{{r_0}^2}{T}. \tag{61}$$

We obtain the same expression as Eq. (60) in the high-temperature limit: for $T \gg E_M$, the resistance is only controlled by ${r_0}^2$.

The approach discussed in this section is limited to temperatures below the plasma frequency ω_p. Above ω_p, the phase delocalizes via thermal activation across the minima of the deep Josephson potential [81], and the resistance increases again until it reaches the insulating regime $R = R_s$ for temperature much larger than E_J.

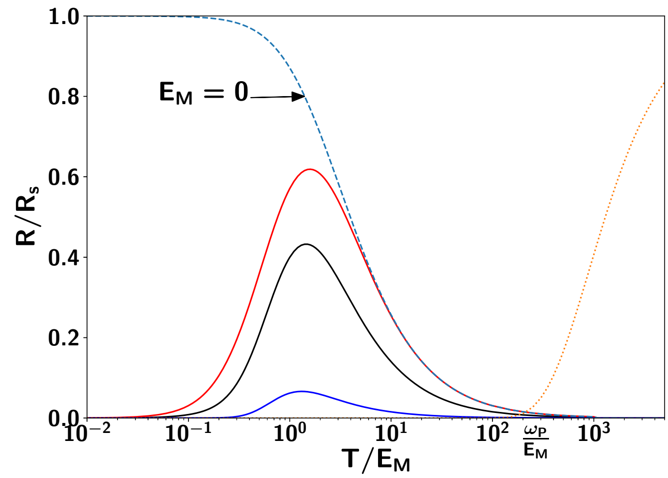

FIG. 7. Resistance vs temperature for ${r_0}^2/2E_M = 0.1$ (blue), 1 (black), and 2 (red), where ${r_0}^2/E_M \sim {t_0}^2/\omega_p E_M$. The limiting case of vanishing E_M is shown in dotted line for comparison. The analysis in this paper is limited to temperatures lower than the plasma frequency ω_p. Above, a thermally activated behavior $\approx e^{-E_J/T}$ towards a full resistance $R = R_s$ occurs [81] (dotted yellow line) corresponding to a complete delocalization of the phase. The subscript ω_p/E_M corresponds to the value where the transition between these two behaviors occurs.

V. CONCLUSION

In this paper, we have considered a superconducting junction with a Josephson energy being the sum of two contributions: the usual 2π-periodic energy and an additional 4π-periodic energy which can be the sign of a topological junction hosting Majorana bound states. The model accounts for a single junction with the two periodicities or, alternatively, two separated Josephson junctions in parallel. The existence of the two commensurate phase periodicities is not necessarily a sign of topology but could also occur with, for instance, a Kondo impurity, a Josephson rhombus device, or in hybrid ferromagnetic-superconducting junctions.

A sufficiently strong shunt resistor in parallel with the junction drives the device via a quantum phase transition to an insulating regime where the zero-temperature Josephson current is suppressed. We have focused on values of the resistance such that the 2π-periodic term alone would give an insulating state while the 4π-periodic energy is still superconducting, resulting in a competition between the two terms. We have derived the corresponding nonmonotonic behavior of the total differential resistance of the device as a function of temperature.

Although our starting point was a compact variable for the phase across the Josephson junction, we proved, using a quantum circuit model for the environment and a suitable gauge transformation, that an extended variable emerges in lieu of the compact phase. This gives a transparent justification to the previous use of an extended phase in the literature [51–53].

For a charging energy much larger than the Josephson energy, the junction is essentially resistive at high temperature. The resistance increases with temperature for

$T > E_C$ but decreases for $T < E_C$, reaching a minimum at $T = T^* \sim E_C$. For even lower temperatures, a crossover towards a fully superconducting junction with zero resistance was established below a local temperature maximum T_m. These features were first derived using perturbation theory and then an exact analytically expression was obtained when $\alpha = 1/2$, or $R_s = 2R_q$. The exact refermionization maps the model onto a helical one-dimensional wire coupled to a topological superconductor.

When the charging energy is the smallest energy scale, we confirmed the nonmonotonic behavior with a tight-binding approach connecting the Josephson wells. Delocalizing the superconducting phase, the hopping between the wells is suppressed by dissipation—by duality, the coupling of the phase to dissipation decreases with the shunt resistance—and a superconducting behavior is restored at low energy. For $\alpha = 1/2$, or $R_s = 2R_q$, we find a mapping to the Emery-Kivelson line of the two-channel Kondo model under finite magnetic field. It provides again an exact expression for the temperature-dependent differential resistance.

A straightforward extension of our paper is the study of the nonlinear current-voltage characteristic where the weight of the Josephson peak is transferred by the environment to higher voltages [24]. Also our analysis is restricted to an equilibrium electromagnetic environment [82] and the prospect of exciting photons around the Josephson junction [83] offers an appealing direction of research.

ACKNOWLEDGMENT

This work has benefited from fruitful discussions with P. Joyez and A. Murani.

APPENDIX A: LINEAR RESPONSE THEORY

We set $E_M = 0$ to simplify the discussion but without loss of generality. The contribution $-I_0(t)\,\hat{\phi}(0)$ in the Hamiltonian (14) can be regarded as a perturbation. We use the framework of linear response theory to compute the voltage drop across the junction. The Kubo formula gives

$$V(t) = \langle\dot{\hat{\phi}}\rangle = i\int_{-\infty}^{t} dt'\,\langle[\dot{\hat{\phi}}(t),\hat{\phi}(t')]\rangle\, I_0(t') \\ = -\int_{-\infty}^{+\infty} dt'\, G^{\text{ret}}_{\dot{\phi},\phi}(t-t')\, I_0(t') \tag{A1}$$

where $\hat{\phi}(t) = \hat{\phi}(x=0,t)$ and the retarded Green's function

$$G^{\text{ret}}(t-t') = -i\theta(t)\langle[\dot{\hat{\phi}}(t),\hat{\phi}(t')]\rangle \tag{A2}$$

where $\theta(t)$ is the Heaviside function. In Fourier space, Eq. (A1) becomes $V(\omega) = -G^{\text{ret}}_{\dot{\phi},\phi}(\omega)\, I_0(\omega)$. $G^{\text{ret}}(\omega)$ is analytical in the upper complex semiplane only. As a consequence, for a real argument ω, the limit $\omega + i0^+$ has to be considered. Now, we use the notation $\phi_0 = 2e\,\hat{\phi}(0)$. With $G^{\text{ret}}_{\dot{\phi},\phi}(\omega) = -i\omega\, G^{\text{ret}}_{\phi,\phi}(\omega)$, the linear resistance is

$$R(\omega) = R_s\,\frac{\alpha}{2\pi}\times i\omega\, G^{\text{ret}}_{\phi_0,\phi_0}(\omega+i0^+). \tag{A3}$$

In the last expression, we have used $1/4e^2 = R_s\,\alpha/2\pi$. To compute $G^{\text{ret}}(\omega+i0^+)$, we compute another correlation function in the imaginary time formalism and do an analytic continuation. We can compute the Matsubara Green's function $G(\tau) = -\langle\mathcal{T}_\tau\phi_0(\tau)\phi_0(0)\rangle$ where $\mathcal{T}_\tau$ is the time ordering. In this paper, we want to compute the DC resistance ($\omega \to 0$) so we need to take the real part of Eq. (A3). The linear resistance becomes

$$\frac{R(T)}{R_s} = -\frac{\alpha}{2\pi}\lim_{\omega\to 0}\text{Re}\bigg[i\omega\lim_{i\omega_n\to\omega+i0^+} \\ \times\int_0^\beta d\tau\, e^{i\omega_n\tau}\,\langle\phi_0(\tau)\phi_0(0)\rangle\bigg]. \tag{A4}$$

In the last expression the time-ordering factor does not appear because the τ is between zero and $\beta > 0$. We can use another expression of (A4) where the correlator is written with Matsubara frequencies:

$$\frac{R(T)}{R_s} = -\frac{\alpha}{2\pi}\lim_{\omega\to 0}\text{Re}\bigg[i\omega\lim_{i\omega_n\to\omega+i0^+} \\ \times\frac{1}{\beta}\sum_{i\omega_k}\langle\phi_0(i\omega_n)\phi_0(i\omega_k)\rangle\bigg]. \tag{A5}$$

The analytical expression of the linear resistance is only determined by the correlator $\langle\phi_0(\tau)\phi_0(0)\rangle$. It can be computed with the Euclidian action [2,6,16,19,84]

$$S = \frac{1}{2\beta}\sum_{i\omega_n}\Big(\frac{1}{8E_C}\,{\omega_n}^2 + \frac{\alpha}{2\pi}\,|\omega_n|\Big)\,|\phi_0(i\omega_n)|^2 \\ - E_J\int_0^\beta d\tau\,\cos\phi_0(\tau) \tag{A6}$$

obtained from Eqs. (14) and (15) in the main text.

In order to have a convenient expression of the correlator, we add to the action (A6) a source term of the form [19]

$$\delta S = \frac{1}{2\beta}\sum_k\Big(\frac{\alpha}{2\pi}|\omega_k| + \frac{1}{8E_C}\,{\omega_k}^2\Big)\,a(-i\omega_k)\,\phi_0(i\omega_k). \tag{A7}$$

Our new action becomes $S_{\text{tot}} = S + \delta S$. We introduce the notation $k_\alpha = \alpha/(2\pi)$ and $k_C = 1/(8E_C)$. With the action S_{tot}, the correlator is

$$\langle\phi_0(i\omega_n)\phi_0(i\omega_k)\rangle = \frac{4\beta^2}{(k_\alpha|\omega_n| + k_C{\omega_n}^2)(k_\alpha|\omega_m| + k_C{\omega_m}^2)} \\ \times\frac{1}{Z}\times\frac{\delta^2 Z}{\delta a(-i\omega_n)\,\delta a(-i\omega_m)}\bigg|_{a=0}. \tag{A8}$$

Before taking the derivatives, it is convenient to perform a shift, $\phi_0(\tau) \to \phi_0(\tau) - a(\tau)/2$. The source term is eliminated and the action S_{tot} is

$$S = \frac{1}{2\beta}\sum_k(k_\alpha\,|\omega_n| + k_C\,{\omega_n}^2)\Big[|\phi_0(i\omega_n)|^2 - \frac{1}{4}\,|a(i\omega_n)|^2\Big] \\ - E_J\int_0^\beta d\tau\,\cos\Big(\phi_0(\tau) - \frac{a(\tau)}{2}\Big). \tag{A9}$$

After taking the derivatives of Eq. (A8), the Matsubara Green's function $G(\tau)$ becomes

$$G(i\omega_n) = -\frac{1}{k_\alpha\,|\omega_n| + k_C\,\omega_n{}^2} - \frac{E_J{}^2}{(k_\alpha\,|\omega_n| + k_C\,\omega_n{}^2)^2} \times \int_0^\beta d\tau\, e^{i\omega_n\tau}\,\langle \mathcal{T}_\tau \sin\phi_0(\tau)\sin\phi_0(0)\rangle. \quad \text{(A10)}$$

We want to compute the DC resistance ($\omega \to 0$). We can drop the k_C term in the last expression. We find

$$\frac{R(T)}{R_{\rm s}} = 1 + \frac{2\pi}{\alpha}\lim_{\omega\to 0}\mathrm{Re}\bigg[\lim_{i\omega_n\to\omega+i0^+}\frac{1}{|\omega_n|} \times \int_0 \beta d\tau\, e^{i\omega_n\tau}\;E_J{}^2\langle\mathcal{T}_\tau \sin\phi_0(\tau)\,\sin\phi_0(0)\rangle\bigg]. \quad \text{(A11)}$$

With $\phi_0 = 2e\,\hat{\phi}(0)$, we find

$$\frac{R(T)}{R_{\rm s}} = 1 + \frac{2\pi}{\alpha}\lim_{\omega\to 0}\mathrm{Re}\bigg[\lim_{i\omega_n\to\omega+i0^+}\frac{1}{|\omega_n|} \times \int_0^\beta d\tau\, e^{i\omega_n\tau}\;E_J{}^2\langle\mathcal{T}_\tau \sin[2e\hat{\phi}(\tau)]\,\sin[2e\hat{\phi}(0)]\rangle\bigg]. \quad \text{(A12)}$$

When $E_M \neq 0$, the calculation is straightforward because the E_J term and the E_M term in Eq. (1) are separated and we find Eqs. (16) and (17).

APPENDIX B: PERTURBATION THEORY FOR THE RESISTANCE

For $E_J \ll E_C$, the Hamiltonian (14) is quadratic. We can use Wick's theorem and obtain Eq. (20):

$$\langle \sin[pe\,\hat{\phi}(\tau)]\,\sin[pe\,\hat{\phi}(0)]\rangle_0 = \tfrac{1}{2}\,e^{J(\tau,p)}. \quad \text{(B1)}$$

The subscript zero means that the average is with respect to the quadratic part of the Hamiltonian (14). For real time and for arbitrary temperature,

$$J(t,p) = \frac{p^2}{2}\int_{-\infty}^{+\infty}\frac{d\omega}{\omega}\,\frac{\mathrm{Re}Z(\omega)}{R_q}\,\frac{e^{-i\omega t} - 1}{1 - e^{-\beta\omega}}. \quad \text{(B2)}$$

In the last expression, we omit the correlator $\langle e^{iep\hat{\phi}(\tau)}\,e^{iep\hat{\phi}(0)}\rangle$ because the exponential goes to zero. For the sake of simplicity, we set $E_M = 0$. It does not change the calculation because only the combinations of E_J and itself and E_M and itself give a nonzero result. The resistance (16) becomes

$$\frac{R}{R_{\rm s}} = 1 + \frac{\pi\,E_J{}^2}{\alpha}\mathrm{Re}\bigg(\frac{i}{\omega}\lim_{i\omega_n\to\omega+i0^+}\int_0^\beta e^{i\omega_n\tau}\;e^{J(\tau,2)}\bigg). \quad \text{(B3)}$$

We can now deform the contour of integration:

$$\int_0^\beta d\tau\, e^{i\omega_n\tau}\;e^{J(\tau,2)} = i\int_0^{+\infty} dt\, e^{-\omega_n t}\;e^{J(t,2)} - i\int_0^{+\infty} dt e^{-\omega_n(t-i\beta)}e^{J(t-i\beta,2)}. \quad \text{(B4)}$$

With $\omega_n\beta = 2\pi n$ and $e^{J(t-i\beta,2)} = e^{J(-t,2)}$, we can make the analytic continuation and find

$$\frac{R(T)}{R_{\rm s}} = 1 - \frac{\pi\,E_J{}^2}{\alpha}\lim_{\omega\to 0}\mathrm{Re}\bigg[\frac{1}{\omega} \times \int_0^{+\infty} dt\, e^{i\omega t}\,(e^{J(t,2)} - e^{J(-t,2)})\bigg]. \quad \text{(B5)}$$

In the DC limit ($\omega \to 0$),

$$\begin{aligned}\frac{R(T)}{R_{\rm s}} &= 1 - \frac{\pi\,E_J{}^2}{\alpha}\mathrm{Re}\bigg[i\int_0^{+\infty} dt\, t(e^{J(t,2)} - e^{J(-t,2)})\bigg] \\ &= 1 - \frac{\pi\,E_J{}^2}{\alpha}\mathrm{Re}\bigg[i\int_{-\infty}^{+\infty} dt\, t\, e^{J(t,2)}\bigg].\end{aligned} \quad \text{(B6)}$$

Instead of integrating along the real axis, we can integrate along the contour swept out by $t - i\beta/2$ for real t. The last expression becomes

$$\begin{aligned}\frac{R(T)}{R_{\rm s}} &= 1 - \frac{\pi\,E_J{}^2\,\beta}{2\alpha}\int_{-\infty}^{+\infty} dt\, e^{J(t-i\beta/2,2)} \\ &= 1 - \frac{\pi\,E_J{}^2\,\beta}{\alpha}\int_0^{+\infty} dt\, e^{J(t-i\beta/2,2)}\end{aligned} \quad \text{(B7)}$$

where

$$J\Big(t - \frac{i\beta}{2}, 2\Big) = j_2(t) = \frac{2}{\alpha}\int_0^{+\infty}\frac{d\omega}{\omega}\times\frac{1}{1 + R_{\rm s}{}^2C^2\omega^2} \times \frac{\cos(\omega t) - \cosh(\beta\omega/2)}{\sinh(\beta\omega/2)}. \quad \text{(B8)}$$

The integration can be performed exactly:

$$j(t,2) = -\frac{2}{\alpha}\bigg[\frac{\pi}{\beta}\Big(t - \frac{i\beta}{2}\Big) + i\pi\,\frac{1 - e^{-\omega_{RC}(t-i\beta/2)}}{1 - e^{i\beta\omega_{RC}}} + \sum_{n=1}^{+\infty}\frac{\omega_{RC}{}^2}{n\,(\omega_{RC}{}^2 - \omega_n{}^2)}\,(1 - e^{-\omega_n\,(t-i\beta/2)})\bigg] \quad \text{(B9)}$$

where $\omega_n = 2\pi n/\beta$ are the Matsubara frequencies and $\omega_{RC} = 1/\tau_{\rm s}$. The sum can be expressed using special functions:

$$\begin{aligned}&\sum_{n=1}^{+\infty}\frac{\omega_{RC}{}^2}{n(\omega_{RC}{}^2 - \omega_n{}^2)}(1 - e^{-\omega_n(t-i\beta/2)}) \\ &= \gamma + \ln(1 + e^{-2\pi t/\beta}) + \frac{1}{2}[\Psi(1-a) + \Psi(1+a)] \\ &\quad - \frac{1}{2}\,e^{-2\pi t/\beta}\,\bigg\{\frac{1}{1-a}\,{}_2F_1(1, 1-a, 2-a, -e^{-2\pi t/\beta}) \\ &\quad + \frac{1}{1+a}\,{}_2F_1(1, 1+a, 2+a, -e^{-2\pi t/\beta})\bigg\}\end{aligned} \quad \text{(B10)}$$

where $a = \beta\omega_{RC}/(2\pi)$, γ is Euler's constant, Ψ is the digamma function, and ${}_2F_1$ is the hypergeometric function. Using $\Psi(1+a) = \Psi(a) + 1/a$ and $\Psi(1-a) = \Psi(a) + \pi\,\mathrm{cotan}\,(\pi a)$ and making the change $y = 2\pi t/\beta$ in the integral (B7), we find

$$\frac{R(T)}{R_{\rm s}} = 1 - \frac{E_J{}^2\,\beta^2}{2\alpha}\int_0^{+\infty} dy\, e^{j_2(y,2\alpha E_C/\pi^2 T)} \quad \text{(B11)}$$

with

$$j_2(y,a) = -\frac{2}{\alpha}\left\{\gamma + \Psi(a) + \ln 2 + \ln \mathrm{ch}\left(\frac{y}{2}\right) + \frac{1}{2}\left[\frac{1}{a} + \frac{\pi\, e^{-ay}}{\sin(\pi a)}\right] - \frac{e^{-y}}{2}\left[\frac{1}{1-a}\,{}_2F_1(1, 1-a, 2-a, -e^{-y}) + \frac{1}{1+a}\,{}_2F_1(1, 1+a, 2+a, -e^{-y})\right]\right\}. \tag{B12}$$

This result can be extended to the case where $E_M \neq 0$ by changing $2/\alpha$ in $1/(2\alpha)$. Finally, we obtain the relation (22).

APPENDIX C: EXPRESSION OF THE S MATRIX

We consider a mode expansion

$$\hat{\psi}(x) = \sum_k (a_k(x)\,\hat{\Gamma}_k + \text{H.c.}), \tag{C1a}$$

$$\hat{\psi}^\dagger(x) = \sum_k (b_k(x)\,\hat{\Gamma}_k + \text{H.c.}), \tag{C1b}$$

$$\hat{a} = \sum_k (u_k\,\hat{\Gamma}_k + \text{H.c.}). \tag{C1c}$$

In the new basis, $\{\hat{\Gamma}_k, \hat{\Gamma}^\dagger_{k'}\} = \delta(k-k')$ and $\{\hat{\Gamma}_k, \hat{\Gamma}_{k'}\} = 0$. In the basis of $\hat{\Gamma}_k$, the Hamiltonian (34) is equal to $H = \sum_k k\,\hat{\Gamma}^\dagger_k\,\hat{\Gamma}_k$. One can obtain a Schrödinger equation for the wave functions $a_k(x)$, $b_k(x)$, and u_k by calculating $[H, \hat{\psi}(x)]$, $[H, \hat{\psi}^\dagger(x)]$, and $[H, \hat{a}]$. We have

$$[H, \hat{\psi}(x)] = i\partial_x\hat{\psi}(x) - 2i\,r_J\,\delta(x)\,\partial_x\hat{\psi}^\dagger(0) + r_M\,\delta(x)\,\hat{a}, \tag{C2a}$$

$$[H, \hat{\psi}^\dagger(x)] = i\partial_x\hat{\psi}^\dagger(x) - 2i\,r_J\,\delta(x)\,\partial_x\hat{\psi}^\dagger(0) - r_M\,\delta(x)\,\hat{a}, \tag{C2b}$$

$$[H, \hat{a}] = r_M\,[\hat{\psi}(0) - \hat{\psi}^\dagger(0)]. \tag{C2c}$$

In the new basis, the system (C2) becomes

$$-k\,a_k(x) = i\,\partial_x a_k - 2ir_J\,\delta(x)\,\partial_x b_k(0) + r_M\,\delta(x)\,u_k, \tag{C3a}$$

$$-k\,b_k(x) = i\partial_x b_k - 2ir_J\,\delta(x)\,\partial_x a_k(0) - r_M\,\delta(x)\,u_k, \tag{C3b}$$

$$-k\,u_k = r_M[a_k(0) - b_k(0)]. \tag{C3c}$$

For $x \neq 0$, the solutions are

$$a_k(x) = e^{i\epsilon_k x}\,[\theta(x)\,a_k^+ + \theta(-x)\,a_k^-], \tag{C4a}$$

$$b_k(x) = e^{i\epsilon_k x}\,[\theta(x)\,b_k^+ + \theta(-x)\,b_k^-] \tag{C4b}$$

where $\theta(x)$ is the Heaviside function and $\epsilon_k = k$. In $x = 0$, we use the following regularizations:

$$a_k(0) = \frac{a_k(0^+) + a_k(0^-)}{2} = \frac{a_k^+ + a_k^-}{2}, \tag{C5a}$$

$$\partial_x a_k(0) = \frac{\partial_x a_k(0^+) + \partial_x a_k(0^-)}{2} = \frac{i\epsilon_k}{2}\,(a_k^+ + a_k^-). \tag{C5b}$$

We have the same expression for the coefficient $b_k(x)$. We can integrate the system (C3) around $x = 0$. Using the boundaries equations (C5), we can express the coefficient a_k^+ with respect to b_k^- and a_k^-:

$$a_k^+ = b_k^-\,\frac{i(2r_J\,{\epsilon_k}^2 + {r_M}^2)}{{r_J}^2{\epsilon_k}^3 + r_J{r_M}^2\,\epsilon_k + \epsilon_k + i{r_M}^2} - a_k^-\,\frac{-{\epsilon_k}^2 + r_J{r_M}^2\,\epsilon_k + {r_J}^2{\epsilon_k}^3}{{r_J}^2{\epsilon_k}^3 + r_J{r_M}^2\,\epsilon_k + \epsilon_k + i{r_M}^2}. \tag{C6}$$

The particle-hole component of the S matrix S_{ph} is the coefficient in front of b_k^-. As a consequence,

$$S_{\text{ph}}(\epsilon_k) = \frac{i(2r_J\,{\epsilon_k}^2 + {r_M}^2)}{{r_J}^2{\epsilon_k}^3 + r_J{r_M}^2\,\epsilon_k + \epsilon_k + i{r_M}^2}. \tag{C7}$$

[1] G.-L. Ingold, Y. V. Nazarov, *Single Charge Tunneling*, edited by H. Grabert, and M. H. Devoret, NATO ASI Series B, Vol. 294 (Springer, Boston, MA, 1992), p. 21.

[2] G. Schon and A. D. Zaikin, Quantum coherent effects, phase transitions, and the dissipative dynamics of ultra small tunnel junctions, Phys. Rep. **198**, 237 (1990).

[3] M. P. A. Fisher and W. Zwerger, Quantum Brownian motion in a periodic potential, Phys. Rev. B **32**, 6190 (1985).

[4] W. Zwerger, Quantum effects in the current-voltage characteristic of a small Josephson junction, Phys. Rev. B **35**, 4737 (1987).

[5] S. Tewari, J. Toner, and S. Chakravarty, Nature and boundary of the floating phase in a dissipative Josephson junction array, Phys. Rev. B **73**, 064503 (2006).

[6] A. Schmid, Diffusion and Localization in a Dissipative Quantum System, Phys. Rev. Lett. **51**, 1506 (1983).

[7] C. P. Herrero and Andrei D. Zaikin, Superconductor-insulator quantum phase transition in a single Josephson junction, Phys. Rev. B **65**, 104516 (2002).

[8] N. Kimura and T. Kato, Temperature dependence of zero-bias resistances of a single resistance-shunted Josephson junction, Phys. Rev. B **69**, 012504 (2004).

[9] H. Kohler, F. Guinea, and F. Sols, Quantum electrodynamic fluctuations of the macroscopic Josephson phase, Ann. Phys. (NY) **310**, 127 (2004).

[10] P. Werner and M. Troyer, Efficient Simulation of Resistively Shunted Josephson Junctions, Phys. Rev. Lett. **95**, 060201 (2005).

[11] S. L. Lukyanov and P. Werner, Resistively shunted Josephson junctions: Quantum field theory predictions versus Monte Carlo results, J. Stat. Mech. (2007) P06002.

[12] R. Yagi, S. Kobayashi, and Y. Ootuka, Phase diagram for superconductor-insulator transition in single small josephson

junctions with shunt resistor, J. Phys. Soc. Jpn. **66**, 3722 (1997).

[13] J. S. Penttila, U. Parts, P. J. Hakonen, M. A. Paalanen, and E. B. Sonin, Superconductor-Insulator Transition in a Single Josephson Junction, Phys. Rev. Lett. **82**, 1004 (1999).

[14] L. S. Kuzmin, Y. V. Nazarov, D. B. Haviland, P. Delsing, and T. Claeson, Coulomb Blockade and Incoherent Tunneling of Cooper Pairs in Ultrasmall Junctions Affected by Strong Quantum Fluctuations, Phys. Rev. Lett. **67**, 1161 (1991).

[15] C. Aslangul, N. Pottier, and D. Saint-James, Quantum Brownian motion in a periodic potential: a pedestrian approach, J. Phys. **48**, 1093 (1987).

[16] S. E. Korshunov, Mobility of a dissipative quantum system in a periodic potential, Zh. Eksp. Teor. Fiz. **93**, 1526 (1987) [Sov. Phys. JETP **65**, 1025 (1987)]

[17] S. Ghoshal and A. B. Zamolodchikov, Boundary S-matrix and boundary state in two-dimensional integrable quantum field theory, Int. J. Mod. Phys. A **9**, 3841 (1999).

[18] S. Qin, M. Fabrizio, and L. Yu, Impurity in a Luttinger liquid: A numerical study of the finite-size energy spectrum and of the orthogonality catastrophe exponent, Phys. Rev. B **54**, R9643 (1996).

[19] C. L. Kane and M. P. A. Fisher, Transmission through barriers and resonant tunneling in an interacting one-dimensional electron gas, Phys. Rev. B **46**, 15233 (1992).

[20] T. Giamarchi, *Quantum Physics in One Dimension* (Oxford University, New York, 2003)

[21] P. Fendley, A. W. W. Ludwig, and H. Saleur, Exact Nonequilibrium dc Shot Noise in Luttinger Liquids and Fractional Quantum Hall Devices, Phys. Rev. Lett. **75**, 2196 (1995).

[22] G.-L. Ingold and H. Grabert, Effect of Zero Point Phase Fluctuations on Josephson Tunneling, Phys. Rev. Lett. **83**, 3721 (1999).

[23] S. Corlevi, W. Guichard, F. W. J. Hekking, and D. B. Haviland, Phase-Charge Duality of a Josephson Junction in a Fluctuating Electromagnetic Environment, Phys. Rev. Lett. **97**, 096802 (2006).

[24] A. Zazunov, N. Didier, and F. W. J. Hekking, Quantum charge diffusion in underdamped Josephson junctions and superconducting nanowires, Europhys. Lett. **83**, 47012 (2008).

[25] A. Kitaev, Unpaired majorana fermions in quantum wires, Phys. Usp. **44**, 131 (2001).

[26] C. W. J. Beenakker, Search for majorana fermions in superconductors, Annu. Rev. Condens. Matter Phys. **4**, 113 (2013).

[27] L. B. Ioffe and M. V. Feigel'man, Possible realization of an ideal quantum computer in Josephson junction array, Phys. Rev. B **66**, 224503 (2002).

[28] N. Read and D. Green, Paired states of fermions in two dimensions with breaking of parity and time-reversal symmetries and the fractional quantum hall effect, Phys. Rev. B **61**, 10267 (2000).

[29] C. Nayak, S. H. Simon, A. Stern, M. Freedman, and S. Das Sarma, Non-Abelian anyons and topological quantum computation, Rev. Mod. Phys. **80**, 1083 (2008).

[30] C. Malciu, L. Mazza, and C. Mora, Braiding Majorana zero modes using quantum dots, Phys. Rev. B **98**, 165426 (2018).

[31] L. P. Rokhinson, X. Liu, and J. J. Furdyna, Observation of the fractional ac Josephson effect: the signature of Majorana particles, Nat. Phys. **1038**, 2429 (2012).

[32] J. Wiedenmann, E. Bocquillon, R. S. Deacon, S. Hartinger, O. Herrmann, T. M. Klapwijk, L. Maier, C. Ames, C. Brune, C. Gould, A. Oiwa, K. Ishibashi, S. Tarucha, H. Buhmann, and L. W. Molenkamp, 4π-periodic Josephson supercurrent in HgTe-based topological Josephson junctions, Nat. Commun. **7**, 10303 (2016).

[33] E. Bocquillon, R. S. Deacon, J. Wiedenmann, P. Leubner, T. M. Klapwijk, C. Brune, K. Ishibashi, H. Buh-mann, and L. W. Molenkamp, Gapless Andreev bound states in the quantum spin Hall insulator HgTe, Nat. Nano. **12**, 137 (2017).

[34] C. Janvier, L. Tosi, L. Bretheau, Ç. Ö Girit, M. Stern, P. Bertet, P. Joyez, D. Vion, D. Esteve, M. F. Goffman, H. Pothier, and C. Urbina, Coherent manipulation of Andreev states in superconducting atomic contacts, Science **349**, 1199 (2015).

[35] D. Golubev, T. Faivre, and J. Pekola, Heat transport through a Josephson junction, Phys. Rev. B **87**, 094522 (2013).

[36] A. Zazunov, S. Plugge, and R. Egger, Fermi Liquid Approach for Superconducting Kondo Problems, Phys. Rev. Lett. **121**, 207701 (2018).

[37] J. A. Ouassou and J. Linder, Spin-switch Josephson junctions with magnetically tunable $\sin(\delta\varphi/n)$ shape, Phys. Rev. B **96**, 064516 (2017).

[38] J. Ulrich, D. Otten, and F. Hassler, Simulation of Supersymmetric Quantum Mechanics in a Cooper-Pair Box Shunted by a Josephson Rhombus, Phys. Rev. Lett. **92**, 245444 (2015).

[39] S. Gladchenko, D. Olaya, E. Dupont-Ferrier, B. Douot, L. B. Ioffe, and M. E. Gershenson, Superconducting nanocircuits for topologically protected qubits, Nat. Phys. **5**, 48 (2009).

[40] M. T. Bell, J. Paramanandam, L. B. Ioffe, and M. E. Gershenson, Protected Josephson Rhombus Chains, Phys. Rev. Lett. **112**, 167001 (2014).

[41] B. Doucot and J. Vidal, Pairing of Cooper Pairs in a Fully Frustrated Josephson Junction Chain, Phys. Rev. Lett. **88**, 227005 (2002).

[42] F. Domínguez, O. Kashuba, E. Bocquillon, J. Wiedenmann, R. S. Deacon, T. M. Klapwijk, G. Platero, L. W. Molenkamp, B. Trauzettel, and E. M. Hankiewicz, Josephson junction dynamics in the presence of 2π- and 4π-periodic supercurrents, Phys. Rev. B **95**, 195430 (2017).

[43] J. Pico-Cortes, F. Dominguez, and G. Platero, Signatures of a 4π-periodic supercurrent in the voltage response of capacitively shunted topological Josephson junctions, Phys. Rev. B **96**, 125438 (2017).

[44] J. D. Sau and F. Setiawan, Detecting topological superconductivity using low-frequency doubled Shapiro steps, Phys. Rev. B **95**, 060501(R) (2017).

[45] Y.-H. Li, J. Song, J. Liu, H. Jiang, Q.-F. Sun, and X. C. Xie, Doubled Shapiro steps in a topological Josephson junction, Phys. Rev. B **97**, 045423 (2018).

[46] P. Matthews, P. Ribeiro, and A. M. Garcia-Garcia, Dissipation in a Topological Josephson Junction, Phys. Rev. Lett. **112**, 247001 (2014).

[47] I. Affleck, M. Oshikawa, and H. Saleur, Quantum brownian motion on a triangular lattice and $c = 2$ boundary conformal field theory, Nucl. Phys. B **594**, 535 (2001).

[48] K. Mullen, D. Loss, and H. T. C. Stoof, Resonant phenomena in compact and extended systems, Phys. Rev. B **47**, 2689 (1993).

[49] S. M. Apenko, Environment-Induced Decompactification of Phase in Josephson Junctions, Phys. Lett. A **142**, 277 (1989).

[50] W. Zwerger, A. T. Dorsey, and M. P. A. Fisher, Effects of the phase periodicity on the quantum dynamics of a resistively shunted josephson junction, Phys. Rev. B **34**, 6518 (1986).

[51] A. Murani, N. Bourlet, H. le Sueur, F. Portier, C. Altimiras, D. Esteve, H. Grabert, J. Stockburger, J. Ankerhold, and P. Joyez, Absence of a Dissipative Quantum Phase Transition in Josephson Junctions, Phys. Rev. X **10**, 021003 (2020).

[52] P. J. Hakonen and E. B. Sonin, Comment on "Absence of a dissipative quantum phase transition in Josephson junctions", Phys. Rev. X **11**, 018001 (2021).

[53] A. Murani, N. Bourlet, H. le Sueur, F. Portier, C. Altimiras, D. Esteve, H. Grabert, J. Stockburger, J. Ankerhold, and P. Joyez, Reply to "Comment on 'Absence of a Dissipative Quantum Phase Transition in Josephson Junctions,"' Phys. Rev. X **11**, 018002 (2021).

[54] J. Koch, V. Manucharyan, M. H. Devoret, and L. I. Glazman, Charging Effects in the Inductively Shunted Josephson Junction, Phys. Rev. Lett. **103**, 217004 (2009).

[55] M. H. Devoret, Quantum fluctuations in electrical circuits, in *Quantum Fluctuations (Les Houches Session LXIII)*, edited by S. Reynaud, E. Giacobino, and J. Zinn- Justin (Elsevier, New York, 1997), pp. 351–386.

[56] J. Leppakangas, G. Johansson, M. Marthaler, and M. Fogelstrom, Input output description of microwave radiation in the dynamical Coulomb blockade, New J. Phys. **16**, 015015 (2014).

[57] J. Kokkala, Quantum computing with itinerant microwave photons, Master's thesis, Aalto University, 2013.

[58] A. Moskova and M. Mosko, Note on the Coulomb blockade of a weak tunnel junction with Nyquist noise: Conductance formula for a broad temperature range, Physica Status Solidi (c) **14**, 1700029 (2016).

[59] H. Grabert and G.-L. Ingold, Mesoscopic Josephson effect, Superlatt. Microstruct. **25**, 915 (1999).

[60] P. Joyez and D. Esteve, Single-electron tunneling at high temperature, Phys. Rev. B **56**, 1848 (1997).

[61] D. Laroche, D. Bouman, D. J. van Woerkom, A. Proutski, C. Murthy, D. I. Pikulin, C. Nayak, R. J. J. van Gulik, J. Nygård, P. Krogstrup, Observation of the 4π-periodic Josephson effect in indium arsenide nanowires, Nat. Commun. **10**, 245 (2019).

[62] C. Mora and K. Le Hur, Probing Dynamics of Majorana Fermions in Quantum Impurity Systems, Phys. Rev. B **88**, 241302(R) (2013).

[63] A. Furusaki and K. A. Matveev, Theory of strong inelastic cotunneling, Phys. Rev. B **52**, 16676 (1995).

[64] H. H. Lin and M. P. A. Fisher, Mode locking in a quantum-Hall-effect point contacts, Phys. Rev. B **54**, 10593 (1996).

[65] L. Fidkowski, J. Alicea, N. H. Lindner, R. M. Lutchyn, and M. P. A. Fisher, Universal transport signatures of Majorana fermions in superconductor-Luttinger liquid junctions, Phys. Rev. B **85**, 245121 (2012).

[66] Z.-W. Zuo, H. Li, L. Li, L. Sheng, R. Shen, and D. Y. Xing, Detecting Majorana fermions by use of superconductor-quantum Hall liquid junctions, Europhys. Lett. **114**, 27001 (2016).

[67] D. I. Pikulin, Y. Komijani, and I. Affleck, Luttinger liquid in contact with a Kramers pair of Majorana bound states, Phys. Rev. B **93**, 205430 (2016).

[68] E. Sela and I. Affleck, Nonequilibrium critical behavior for electron tunneling through quantum dots in an Aharonov-Bohm circuit, Phys. Rev. B **79**, 125110 (2009).

[69] U. Weiss and M. Wollensak, Dynamics of the dissipative multiwell system, Phys. Rev. B **37**, 2729 (1988).

[70] J. Koch, T. M. Yu, J. Gambetta, A. A. Houck, D. I. Schuster, J. Majer, A. Blais, M. H. Devoret, S. M. Girvin, and R. J. Schoelkopf, Charge-insensitive qubit design derived from the Cooper pair box, Phys. Rev. A **76**, 042319 (2007).

[71] S. A. Wilkinson, N. Vogt, D. S. Golubev, and J. H. Cole, Approximate solutions to Mathieu's equation, Physica E Low dimens. Syst. Nanostruc. **100**, 24 (2018).

[72] G. Catelani, R. J. Schoelkopf, M. H. Devoret, and L. I. Glazman, Relaxation and frequency shifts induced by quasiparticles in superconducting qubits, Phys. Rev. B **84**, 064517 (2011).

[73] K. Yavilberg, E. Ginossar, and E. Grosfeld, Fermion parity measurement and control in Majorana circuit quantum electrodynamics, Phys. Rev. B **92**, 075143 (2015).

[74] E. Ginossar and E. Grosfeld, Microwave transitions as a signature of coherent parity mixing effects in the Majorana-transmon qubit, Nat. Commun. **5**, 4772 (2014).

[75] J. R. Johansson, P. D. Nation, and F. Nori, QuTiP: An open-source Python framework for the dynamics of open quantum systems, Comput. Phys. Commun. **183**, 1760 (2012).

[76] J. R. Johansson, P. D. Nation, and F. Nori, QuTiP 2: A Python framework for the dynamics of open quantum systems, Comput. Phys. Commun. **184**, 1234 (2013).

[77] J. K. Asboth, L. Oroszlany, and A. P. Palyi, *A Short Course on Topological Insulators: Band Structure and Edge States in One and Two Dimensions*, Lecture Notes in Physics (Springer, New York, 2016).

[78] M. Mancini, Fermionization of spin systems, Ph.D. thesis, Università degli Studi di Perugia, 2008.

[79] V. J. Emery and S. Kivelson, Mapping of the two-channel Kondo problem to a resonant-level model, Phys. Rev. B **46**, 10812 (1992).

[80] A. M. Sengupta and A. Georges, Emery-Kivelson solution of the two-channel Kondo problem, Phys. Rev. B **49**, 10020 (1994).

[81] P. Nozieres and G. Iche, Brownian motion in a periodic potential under an applied bias: The transition from hopping to free conduction, J. Phys. (Paris) **40**, 225 (1979).

[82] E. G. Dalla Torre, E. Demler, T. Giamarchi, and E. Altman, Dynamics and universality in noise-driven dissipative systems, Phys. Rev. B **85**, 184302 (2012).

[83] U. C. Mendes and C. Mora, Cavity squeezing by a quantum conductor, New J. Phys. **17**, 113014 (2015).

[84] G. Falci, V. Bubanja, and G. Schon, Quasiparticle and Cooper pair tunneling in small capacitance Josephson junctions, Z. Phys. B **85**, 451 (1991).